

Comparative study of enhancement and suppression of N_2^+ lasing induced by coherent molecular rotational wave packets of N_2 and N_2^+

Hongqiang Xie^{1,2,*}, Shuting Wu,² Yihong Huang,² Junda Lv,¹ Jiayi Cai,¹ Chenrui Jing,^{3,†}
Zaicheng Xiao,¹ Zhiming Chen,¹ Xinghao Wang,¹ and Guihua Li^{2,‡}

¹*School of Science, East China University of Technology, Nanchang 330013, China*

²*School of Science, East China Jiaotong University, Nanchang 330013, China*

³*Department of Physics, Luoyang Normal University, Luoyang 471934, China*



(Received 7 January 2024; accepted 8 March 2024; published 1 April 2024)

N_2^+ lasing action involves the creation, evolution, and radiation of ions in intense laser fields. In this paper, we demonstrate that N_2^+ lasing intensity can be enhanced by several times or totally suppressed by controlling the ionic creation and radiation processes through manipulation of the coherent molecular rotational wave packets of N_2 and N_2^+ with a pump-control scheme. Our results show that if a weak control pulse arrives at the revival moments of the ionic rotational wave packet, the lasing signal can be notably promoted, which is in contrast to observations in previous studies. Meanwhile, the modulation profiles of the lasing signals caused by molecular alignments of N_2 and N_2^+ are analyzed at length, revealing the double roles of the weak control pulse in inducing molecular alignment of N_2 or monitoring the amplification of the N_2^+ system by controlling electronic and rotational coherence. Moreover, by performing a Fourier transformation of the delay-dependent N_2^+ lasing, the rotational wave-packet information of N_2 and N_2^+ is simultaneously retrieved.

DOI: [10.1103/PhysRevA.109.043101](https://doi.org/10.1103/PhysRevA.109.043101)

I. INTRODUCTION

Small molecules exposed to an intense femtosecond laser field can be partially ionized, and the created molecular ions, together with the unionized neutral molecules, will be rotationally excited in a coherent fashion, resulting in the well-known field-free molecular alignment at subsequent revival moments. Molecular alignment has been extensively investigated in many strong-field pump-probe experiments, such as molecular ionization [1], high harmonic generation [2], and orbital imaging [3], etc., in the past few decades. Accordingly, many spectroscopic techniques including angle-resolved photoelectron spectroscopy [4], high harmonic spectroscopy [5], and polarization spectroscopy [6] have been explored to retrieve molecular rotational wave-packet information. The revival periods for neutral molecules and cations are usually close to each other since the removal of one electron could not significantly change the rotational inertia of molecules. None of the proposed spectroscopic techniques or approaches allow us to concurrently decode the molecular rotational wave packets of both neutral molecules and ions, which is critical to unravel the relevance of these two wave packets because of ionization.

Recently developed N_2^+ lasing spectroscopy offers an alternative means to study molecular rotational behaviors [7–11]. The mechanism of N_2^+ lasing has been widely studied in recent years, showing that multiple different gain and amplification routes can take effect [12–22]. N_2^+ lasing action involves the ionic creation, evolution within the pump laser

field, and radiation after the pump. The birth rate of ions is related to the angle of the molecular axis relative to the laser polarization direction, and the evolution and radiation processes determined by the ionic polarizability are frequently manipulated to control the resulting ionic emission intensity. Previous studies have achieved the molecular alignment of neutral molecules with few-cycle femtosecond pulses [23] or alignment information of ions by the use of a two-color scheme [7]. Unfortunately, the existing schemes also fail to decouple simultaneously the rotational wave packets of N_2 and N_2^+ .

In the present paper, we simultaneously achieve the rotational-state distribution information of the coherent rotational wave packets of N_2 and N_2^+ by single scanning the relative delay between a strong 800-nm pump and a weak 800-nm control pulse. This permits us directly to discern the variation of rotational distribution due to ionization and the subsequent excitation. In addition, direct modulation comparisons induced by N_2 and N_2^+ alignments in N_2^+ lasing provide critical guidance on how to better optimize the lasing efficiency using molecular rotational wave packets. Equally importantly, we also discussed the enhancement and suppression mechanism thereof. We noticed that the quantum erasing mechanism has been proposed to interpret the suppression of N_2^+ lasing [24], which is not appropriate for explaining the enhancement effect of the N_2^+ lasing signal in our case. Our findings emphasize the combined contributions of electronic and rotational coherence to control the gain of N_2^+ lasing.

II. EXPERIMENTAL

The experiments were carried out with a commercial Ti:sapphire laser system delivering 800-nm femtosecond laser

*xhq3126336@sina.com

†jinglytree@163.com

‡qingshafeihua@163.com

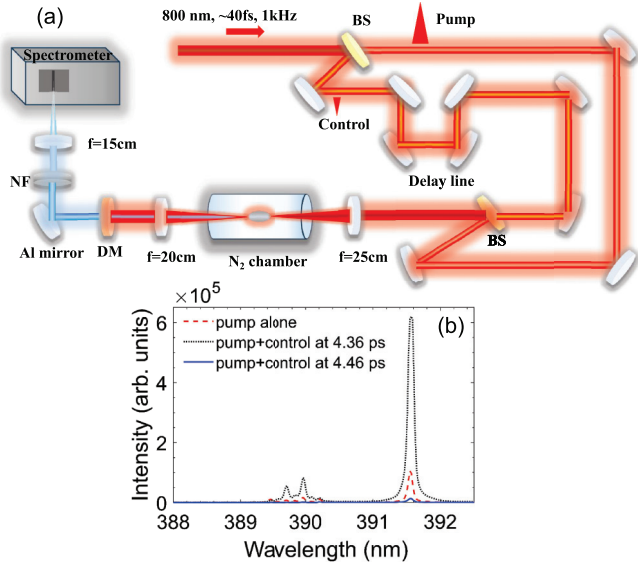


FIG. 1. (a) The pump-control experimental setup. BS: beam splitter; DM: dichroic mirror; NF: neutral filter. (b) The typical spectra of N_2^+ lasing at 391.4 nm for several pump-control delays of 4.36 and 4.46 ps. The lasing spectrum induced by the pump only is plotted for comparison.

pulses with a maximum energy of 7 mJ and a duration of ~ 40 fs at a repetition rate of 1 kHz. As illustrated in Fig. 1(a), the output femtosecond pulses from the laser system were first divided into two parts. One beam with an energy of 1.6 mJ acted as the strong pump pulse responsible for ionization and inducing N_2^+ lasing. The other beam with an energy of 0.16 mJ served as the weak control pulse employed to monitor the creation of N_2^+ lasing. The pump and control pulses are linearly polarized along the same direction. The time interval between these two beams can be finely controlled with a motorized translation stage with a minimum step of 0.002 mm. Both beams are focused by an $f = 25$ cm lens after being combined in a gas chamber filled with pure nitrogen gas. The diameter of the incident pump and control pulses is ~ 7 mm at $1/e^2$ of the maximum intensity. The peak laser intensity of the pump and control pulses achieved by tight focusing conditions assuming a linear propagation can reach $\sim 4 \times 10^{15}$ and $\sim 4 \times 10^{14}$ W/cm², respectively. The actual focusing intensity could be much smaller due to the plasma defocusing effect [14]. The forward N_2^+ lasing exiting from the chamber after collimation by an $f = 20$ cm lens and separation from the intense 800-nm pump laser with two dichroic mirrors (high reflectivity at ~ 800 nm and high transmission at ~ 400 nm) is focused onto the entrance slit of a grating spectrometer (Andor Shamrock 500i) equipped with an intensified charge-coupled device (ICCD). The entrance slit of the spectrometer was adjusted to be 100 μ m and the exposure time was 50 ms.

III. RESULTS

Figure 1(b) shows comparative N_2^+ lasing spectra at 391.4 nm [that can be assigned to the transition between $B^2\Sigma_u^+(v=0)$ and $X^2\Sigma_g^+(v=0)$] generated in 5 mbar N_2 for pump-control delays of 4.36 and 4.46 ps. Positive (negative) delay means the pump (control) pulse arrives in the gas

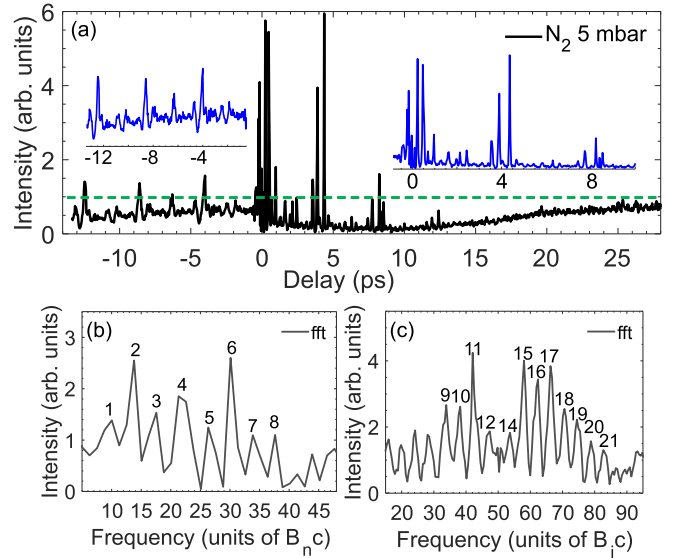


FIG. 2. (a) The signal intensity of N_2^+ lasing at 391.4 nm as a function of the time interval between the strong pump and weak control pulses at a pressure of 5 mbar N_2 . The delay-dependent N_2^+ lasing intensity is scaled by that created by the pump only (see the green straight line). Positive delay means the pump pulse precedes the control pulse. Two zoomed windows of -13.6 to -0.5 ps and -1 to 10 ps are shown as insets for resolving the modulation structures caused by molecular alignments. The Fourier transform spectra of N_2^+ lasing for the negative and positive delay windows are respectively depicted in (b) and (c).

chamber first and the zero delay is determined by observing the strongest interference of these two pulses. It can be seen that the lasing intensity is enhanced at 4.36 ps and suppressed at 4.46 ps, in comparison to that produced by the pump only (the red curve). We will analyze the origins thereof later.

Figure 2(a) shows the P -branch intensity of N_2^+ lasing at 391.4 nm as a function of the time delay between the pump and control pulses at a pressure of 5 mbar. Note that the lasing intensity has been normalized by the signal (represented by the green straight curve) generated by the pump alone for analyzing the enhancement and suppression effects. The first interesting observation can be spotted in the figure is that the lasing signals are modulated at several specific delay moments along the negative and positive x axis. The detailed structures of these modulations caused by molecular alignments can be found in the insets of Fig. 2(a). The left and right revival structures display an obvious difference, which is related to the different roles of the weak control pulse in these two cases and will be discussed in detail later. The rotational periods of N_2 and N_2^+ are respectively ~ 8.4 ps [23] and ~ 8 ps [7]. We further perform the fast Fourier transformation for the data of N_2^+ lasing in the negative and positive delay range. The results are respectively presented in Figs. 2(b) and 2(c), showing that the modulation of lasing signals within the negative x axis is in line with the molecular rotational wave packet of neutral N_2 while the lasing signal within the positive x axis is consistent with the molecular rotational wave packet of N_2^+ on the $B^2\Sigma_u^+$ state [8,25]. The rotational constant B_n of neutral N_2 on the ground state is 1.989 cm⁻¹ [23] and the rotational constant

B_i of N_2^+ on the $B^2\Sigma_u^+$ state is 2.073 cm^{-1} [8,26]. The numbers on each peak denote the rotational states consisting of the corresponding wave packet. It can be seen that the highest populated rotational state in the neutral wave packet is $J = 8$ while the highest population-inverted state in the ionic wave packet reaches $J = 21$. In addition, it deserves mentioning that the rotational state $J = 13$ cannot be observed in the wave packet of N_2^+ , which has been elaborately explained in our previous works [8,26]. It is due to nearly the same population modulation frequency for the upper rotational state $J = 13$ on the $B^2\Sigma_u^+(\nu = 0)$ and the lower rotational state $J = 14$ on the $X^2\Sigma_g^+(\nu = 0)$. The difference in their modulation frequencies leads to the vanishing signal at a frequency of $J = 13$.

Another interesting observation in Fig. 2(a) concerns the enhancement and suppression of N_2^+ lasing. First, when the pump pulse lags behind the control pulse, the lasing signal is indistinguishably suppressed except around the alignment moments of N_2 to a certain extent, which can be attributed to the plasma influence brought about by the weak ionization of the control pulse. This suppression effect can sustain within the whole plasma lifetime [24]. Second, when the pump pulse is prior to the control pulse, the lasing signal except at the alignment delays of N_2^+ first decreases with increments of the pump-control delay and reaches a minimum around ~ 9 ps, and then starts to rise gradually until approaching the intensity created by the pump only. The suppression is due to the decreased polarization between the electronic-vibrational states of $B^2\Sigma_u^+(\nu = 0)$ and $X^2\Sigma_g^+(\nu = 0)$ caused by the resonant electronic couplings between the $X^2\Sigma_g^+$ and $A^2\Pi_u$ states [19]. It is noteworthy that according to the superradiance picture [13,22], the appearance of a lasing signal should be temporally retarded with respect to the initial pump pulse, depending on the gas pressure and the triggering intensity [13,22]. In our case, the moment (~ 9 ps) for observing the minimum lasing is in accord with the birth time of N_2^+ lasing, according to the experimental results in Ref. [13]. Therefore, the growing process in Fig. 2(a) after a delay time ~ 9 ps in fact reflects the creation process of N_2^+ lasing generated by the pump alone. Additionally, it can be seen that the lasing signal can be greatly enhanced at the revival moments of N_2^+ . Note that the enhancement of N_2^+ lasing enabled by the molecular alignment of N_2^+ cannot be accomplished in the previous similar work of Ref. [24]. A different explanation for the enhancement and suppression mechanism is proposed in the following.

To further uncover the suppression dynamics of N_2^+ lasing caused by the weak control pulse, we performed the same measurements at pressures of 30, 50, and 70 mbar. The results are presented in Fig. 3. It can be seen that when the control pulse arrives before the pump pulse, similar modulation shapes at the revival moments of N_2 are observed while the suppression induced by the plasma effect is more significant for the case of 70 mbar, in comparison to that for the cases of 30 and 50 mbar. The possible origins thereof are the relatively high plasma density at 70 mbar and the detrimental impact on propagation of the follow-up pump laser. In addition, when the control pulse lags behind the pump, minimum lasing moments occur at ~ 3 , ~ 2.2 , and ~ 1.6 ps for pressures of 30, 50, and 70 mbar, respectively. The falling edges of these three

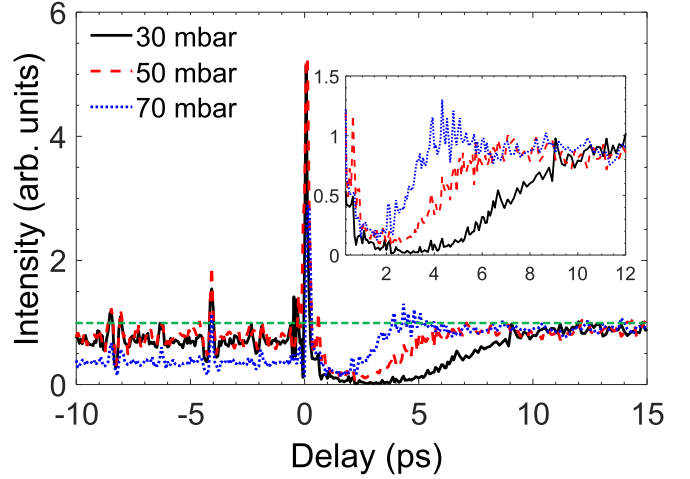


FIG. 3. (a) N_2^+ lasing intensity normalized by a lasing signal produced by the pump alone varies with the pump-control delay at several pressures of 30, 50, and 70 mbar. The inset shows the corresponding variation of lasing within the time window of 0.3–12 ps.

curves are nearly the same while the rising edge becomes more steep with increasing pressure. Moreover, the ionic rotational wave packet fails to enhance the N_2^+ lasing at the revival moments for the three pressures, differing from the results shown in Fig. 2(a).

It deserves mentioning that due to the sufficient pump laser intensity at the focus the electronic population inversion between the $B^2\Sigma_u^+(\nu = 0)$ and $X^2\Sigma_g^+(\nu = 0)$ states with the assistance of the $A^2\Pi_u$ state can be readily achieved [14,15] and is the main gain origin. Meanwhile, the amplification mechanism is in essence superradiance [11,13,19,22,27]. Note that the two-photon process with inversion between the $B^2\Sigma_u^+$ and $A^2\Pi_u$ states unlikely occurs due to the mismatch between the driving wavelength and two-photon transition wavelength. In addition, the transient inversion mechanism in the vicinity of the alignment delays of N_2^+ due to the different rotational constants of $B^2\Sigma_u^+(\nu = 0)$ and $X^2\Sigma_g^+(\nu = 0)$ was first proposed by Kartashov *et al.* [28] and the coherent rotational dynamics can be reflected by the time-domain measurement using the cross-correlation frequency-resolved optical gating (X-FROG) technique, which cannot explain the light amplification at nonalignment delays and thus can be precluded.

IV. DISCUSSIONS

Simultaneously mapping the rotational wave packets of neutral molecules and cations is beneficial to understanding the rotational excitation process arising from ionization. The N_2^+ lasing spectrum exhibits some advantages over other strong-field spectroscopic techniques in this regard. Here, we observed two alignment effects occurring in the intensity modulation of N_2^+ lasing while tuning the time interval of a strong 800-nm pump and a weak 800-nm control pulse. Through Fourier transform spectra of N_2^+ lasing, the spectrally resolved rotational states consisting of N_2 and N_2^+ rotational wave packets are obtained. It is noteworthy that the Fourier transformed spectroscopy provides a better spectral

resolution than that of the adopted spectrometer, even permitting us to identify the missing rotational-state lasing of $J = 13$ in the ionic rotational wave packet, as shown in Fig. 2(c).

The different modulation shapes of N_2^+ lasing caused by molecular alignments of N_2 and N_2^+ indicate the different roles of the weak control pulse. When the control pulse arrives before the pump, it induces the molecular alignment of N_2 , which influences the ionization process of the subsequent strong pump pulse that impinges on the molecules at the revival moments. The ionization probability is maximized when the molecules are aligned along the pump laser polarization direction and hence the optimized lasing signal can be obtained. However, when molecules are aligned perpendicular to the pump laser polarization, the ionization is least efficient and results in a minimum of N_2^+ lasing. So alignment-dependent ionization causes modulation profiles of N_2^+ lasing similar to the molecular alignment of N_2 . For the case of the pump pulse preceding the control pulse, the weak control pulse may not only disturb the quantum coherence between the states of $B^2\Sigma_u^+(\nu = 0)$ and $X^2\Sigma_g^+(\nu = 0)$ via resonant electronic couplings between the $X^2\Sigma_g^+(\nu = 0)$ and $A^2\Pi_u(\nu = 2)$ states [19], but also can change the population inversion between the states of $B^2\Sigma_u^+(\nu = 0)$ and $X^2\Sigma_g^+(\nu = 0)$ via population transfer [14,15]. We can see that the lasing signal at the revival moments of N_2^+ appears as a multiple-peak structure, such as at 4 ps, which corresponds to the rotational dynamics of the $B^2\Sigma_u^+(\nu = 0)$ state according to the Fourier transform spectrum in Fig. 2(c). First, at the alignment delays of N_2^+ , the electronic couplings between the $X^2\Sigma_g^+(\nu = 0)$ and $A^2\Pi_u(\nu = 2)$ states are prohibited due to the perpendicular transition property, and the weak control pulse can reinforce the alignment of N_2^+ on the $B^2\Sigma_u^+(\nu = 0)$ and $X^2\Sigma_g^+(\nu = 0)$ states, facilitating the establishment of macroscopic quantum coherence among N_2^+ emitters and leading to a significant enhancement of the superradiant lasing signal. Second, at the antialignment delays of N_2^+ , the disruption of electronic coherence between the states of $B^2\Sigma_u^+(\nu = 0)$ and $X^2\Sigma_g^+(\nu = 0)$ is the strongest. The serious disturbance of the electronic coherence results in completely suppressed lasing. But due to the small baseline near 4 ps, obvious dips are barely observed at the antialignment delays. The above two factors cause the observed multiple-peak structure near the alignment moments of N_2^+ .

It is noteworthy that the measured revival structures caused by N_2^+ rotational wave packet with our pump-control scheme is different from that obtained by a typical two-color scheme [7,26], where a postponed seed pulse is introduced to directly induce N_2^+ lasing and results in the signal modulation similar to the molecular alignment of N_2^+ . In addition, we note that an adaptive control scheme dedicated to optimization of the ionization and excitation processes during N_2^+ lasing generation using sequential femtosecond pulses in a high-pressure gas cell was put forward by Kartashov *et al.*, which results in a significant enhancement of N_2^+ lasing lines at 358, 391, and 428 nm [29].

The lasing intensity variation within the positive delays for the three pressures in Fig. 3 can be interpreted as follows. When the pump pulse precedes the control pulse, it can create ionization, rotational excitation, and self-seeding amplification of N_2^+ lasing. According to our previous investigations [22,27], there exists a certain delay between the N_2^+ lasing and the pump pulse required for establishing macroscopic quantum coherence for producing superradiance [13,22]. The delayed control pulse can destroy the building up process of macroscopic quantum coherence, leading to similar falling edges within the positive delays for the three curves depicted in Fig. 3. Note that the disturbance caused by the control pulse becomes stronger with increasing pump-control delay before generation of N_2^+ lasing emission since the macroscopic quantum coherence increases within the delays. The moments observing minimum lasing signals for the three cases in Fig. 3 reflect the retarded time required for constructing macroscopic quantum coherence, which shortens with increasing pressure and basically complies with the superradiance picture. The whole rising edges in the three curves of Fig. 3 are associated with the duration of N_2^+ lasing, which increases with decreasing pressure, as demonstrated in several previous works [13,22]. Moreover, the almost imperceptible modulations induced by the ionic alignments in Fig. 3 is due to the fact that the revival moments can temporally overlap the radiation process of N_2^+ system due to the shortened retarded time required for establishing the macroscopic quantum coherence. At this time, the arrival of the control pulse could not arouse the apparent variation of the macroscopic quantum coherence due to the reduced electronic coherence and the population on the upper level.

V. CONCLUSIONS

To conclude, we systematically investigated the essential roles of molecular alignment of N_2 and N_2^+ naturally induced by ubiquitous 800-nm femtosecond lasers in controlling N_2^+ lasing, by which the information of two rotational wave packets is simultaneously decoded. Our results demonstrate the former can be utilized to manipulate the ionization process and the latter can be employed to control the radiation process of N_2^+ . The enhancement and suppression mechanism is discussed at length, revealing the crucial role of electronic coherence in enhancing the lasing signal at the revival moments of ionic alignment. The combined quantum effects of the electronic and rotational coherence in the enhancement of N_2^+ lasing is invalid at a high gas pressure or under real filamentation conditions when the ionization of N_2 becomes difficult. Our findings thus shed light on the manipulation of N_2^+ lasing by using electronic and rotational coherence.

ACKNOWLEDGMENTS

This work is supported by the National Natural Science Foundation of China (No. 12074063, No. 12064009, No. 12264003, and No. 12264002) and the Jiangxi Provincial Natural Science Foundation (No. 20232ACB211007, No. 20212BAB211008, and No. 20232BAB201041).

- [1] D. Pavičić, K. F. Lee, D. M. Rayner, P. B. Corkum, and D. M. Villeneuve, *Phys. Rev. Lett.* **98**, 243001 (2007).
- [2] J. Itatani, D. Zeidler, J. Levesque, M. Spanner, D. M. Villeneuve, and P. B. Corkum, *Phys. Rev. Lett.* **94**, 123902 (2005).
- [3] J. Itatani, J. Levesque, D. Zeidler, H. Niikura, H. Pépin, J. Kieffer, P. Corkum, and D. Villeneuve, *Nature (London)* **432**, 867 (2004).
- [4] A. Stolow, A. Bragg, and D. Neumark, *Chem. Rev.* **104**, 1719 (2004).
- [5] L. He, S. Sun, P. Lan, Y. He, B. Wang, P. Wang, X. Zhu, L. Li, W. Cao, P. Lu, and C. Lin, *Nat. Commun.* **13**, 4595 (2022).
- [6] V. Renard, O. Faucher, and B. Lavorel, *Opt. Lett.* **30**, 70 (2005).
- [7] H. Zhang, C. Jing, J. Yao, G. Li, B. Zeng, W. Chu, J. Ni, H. Xie, H. Xu, S. L. Chin, K. Yamanouchi, Y. Cheng, and Z. Xu, *Phys. Rev. X* **3**, 041009 (2013).
- [8] H. Xie, B. Zeng, G. Li, W. Chu, H. Zhang, C. Jing, J. Yao, J. Ni, Z. Wang, Z. Li, and Y. Cheng, *Phys. Rev. A* **90**, 042504 (2014).
- [9] A. Azarm, P. Corkum, and P. Polynkin, *Phys. Rev. A* **96**, 051401(R) (2017).
- [10] L. Arissian, B. Kamer, A. Rastegari, D. M. Villeneuve, and J. C. Diels, *Phys. Rev. A* **98**, 053438 (2018).
- [11] H. Xie, H. Lei, G. Li, Q. Zhang, X. Wang, J. Zhao, Z. Chen, J. Yao, Y. Cheng, and Z. Zhao, *Phys. Rev. Res.* **2**, 023329 (2020).
- [12] J. Yao, B. Zeng, H. Xu, G. Li, W. Chu, J. Ni, H. Zhang, S. L. Chin, Y. Cheng, and Z. Xu, *Phys. Rev. A* **84**, 051802(R) (2011).
- [13] Y. Liu, P. Ding, G. Lambert, A. Houard, V. Tikhonchuk, and A. Mysyrowicz, *Phys. Rev. Lett.* **115**, 133203 (2015).
- [14] H. Xu, E. Lötstedt, A. Iwasaki, and K. Yamanouchi, *Nat. Commun.* **6**, 8347 (2015).
- [15] J. Yao, S. Jiang, W. Chu, B. Zeng, C. Wu, R. Lu, Z. Li, H. Xie, G. Li, C. Yu, Z. Wang, H. Jiang, Q. Gong, and Y. Cheng, *Phys. Rev. Lett.* **116**, 143007 (2016).
- [16] M. Britton, P. Laferriere, D. H. Ko, Z. Li, F. Kong, G. Brown, A. Naumov, C. Zhang, L. Arissian, and P. B. Corkum, *Phys. Rev. Lett.* **120**, 133208 (2018).
- [17] X. Zhang, Q. Lu, Z. Zhang, Z. Fan, D. Zhou, Q. Liang, L. Yuan, S. Zhuang, K. Dorfman, and Y. Liu, *Optica* **8**, 668 (2021).
- [18] A. Mysyrowicz, R. Danylo, A. Houard, V. Tikhonchuk, X. Zhang, Z. Fan, Q. Liang, S. Zhuang, L. Yuan, and Y. Liu, *APL Photonics* **4**, 110807 (2019).
- [19] A. Zhang, Q. Liang, M. Lei, L. Yuan, Y. Liu, Z. Fan, X. Zhang, S. Zhuang, C. Wu, Q. Gong, and H. Jiang, *Opt. Express* **27**, 14922 (2019).
- [20] H. Lei, J. Yao, J. Zhao, H. Xie, F. Zhang, H. Zhang, N. Zhang, G. Li, Q. Zhang, X. Wang, Y. Yang, L. Yuan, Y. Cheng, and Z. Zhao, *Nat. Commun.* **13**, 4080 (2022).
- [21] Q. Zhang, H. Xie, G. Li, X. Wang, H. Lei, J. Zhao, Z. Chen, J. Yao, Y. Cheng, and Z. Zhao, *Commun. Phys.* **3**, 50 (2020).
- [22] H. Xie, H. Lei, G. Li, J. Yao, Q. Zhang, X. Wang, J. Zhao, Z. Chen, Y. Cheng, and Z. Zhao, *Photonics Res.* **9**, 2046 (2021).
- [23] H. Xu, E. Lötstedt, T. Ando, A. Iwasaki, and K. Yamanouchi, *Phys. Rev. A* **96**, 041401(R) (2017).
- [24] R. Danylo, G. Lambert, Y. Liu, V. Tikhonchuk, A. Houard, and A. Mysyrowicz, *Opt. Lett.* **45**, 4670 (2020).
- [25] Y. Zhang, E. Lötstedt, T. Ando, A. Iwasaki, H. Xu, and K. Yamanouchi, *Phys. Rev. A* **104**, 023107 (2021).
- [26] B. Zeng, W. Chu, G. Li, J. Yao, H. Zhang, J. Ni, C. Jing, H. Xie, and Y. Cheng, *Phys. Rev. A* **89**, 042508 (2014).
- [27] G. Li, C. Jing, B. Zeng, H. Xie, J. Yao, W. Chu, J. Ni, H. Zhang, H. Xu, Y. Cheng, and Z. Xu, *Phys. Rev. A* **89**, 033833 (2014).
- [28] D. Kartashov, S. Haessler, S. Ališauskas, G. Andriukaitis, A. Pugžlys, A. Baltuška, J. Möhring, D. Starukhin, M. Motzkus, A. M. Zheltikov, M. Richter, F. Morales, O. Smirnova, M. Y. Ivanov, and M. Spanner, in *Research in Optical Sciences*, OSA Technical Digest (Optica Publishing Group, Washington, DC, 2014).
- [29] D. Kartashov, J. Möhring, G. Andriukaitis, A. Pugžlys, A. Zheltikov, M. Motzkus, and A. Baltuška, in *Conference on Lasers and Electro-Optics 2012*, OSA Technical Digest (Optica Publishing Group, Washington, DC, 2012).